

# Statistics of Particle Trajectories at Short Time-Intervals Reveal Electrostatic Colloidal Interactions in Nonpolar Solvents

Sunil K. Sainis, Vincent Germain, and Eric R. Dufresne

*Departments of Mechanical Engineering, Chemical Engineering and Physics, Yale University, New Haven, CT 06511.\**

(Dated: May 26, 2019)

Interparticle forces play an essential role in determining the properties of colloidal suspensions. We describe and implement a technique to measure the electrostatic forces of polymer microspheres suspended in nonpolar microemulsions. This method is not limited to colloidal systems, but can extract forces from the relaxation of any overdamped thermal system with normal modes. At sufficiently short time-intervals, the evolution of a normal mode is well described by a one-dimensional Smoluchowski equation with constant drift velocity,  $v$ , and diffusion coefficient,  $D$ . By virtue of fluctuation-dissipation, these transport coefficients are simply related to conservative forces,  $F$ , acting on the normal mode:  $F = k_B T v / D$ . This relationship implicitly accounts for hydrodynamic interactions, requires no mechanical calibration, makes no assumptions about the form of conservative forces, and requires no prior knowledge of material properties.

PACS numbers: 82.70.Dd, 82.70.Uv

The structure and stability of colloidal dispersions depend sensitively on the interactions of suspended particles. An early triumph of colloid science was the theory of Derjaguin-Landau-Verwey and Overbeek (DLVO) [1, 2] which juxtaposes short-range Van der Waals forces and longer-range electrostatic forces to characterize the stability of aqueous colloidal dispersions. On the other hand, the role of electrostatic interactions in nonpolar solvents has remained controversial [3]. Electrostatic forces between surfaces in nonpolar solvents have recently been reported for a variety of surfaces in nonpolar microemulsions [4, 5, 6]. In certain regimes, measured interactions [6] are identical to the screened-Coulomb component of the standard DLVO theory. In others, a novel counterion-only double-layer theory is needed to describe observed forces [7]. While the reality of electrostatic interactions in nonpolar environments has become established, their origin and significance remain mysterious. To that end, robust methods for measuring interparticle forces are needed to bring out the underlying physics.

A variety of methods have emerged to directly measure colloidal forces. The surface forces apparatus [4, 8] and atomic force microscope [5, 9] measure forces directly and have respective force resolutions at the nN and pN scales. Alternatively, native thermal fluctuations can reveal interparticle forces. Such methods are well suited to real-space imaging and provide force resolutions on the fN scale. For one-dimensional and/or weakly interacting systems, the potential can be extracted from the equilibrium distribution [10, 11] by inverting the Boltzmann equation  $U/k_B T = -\ln P_{eq}$ . Similarly, liquid-structure theory or reverse Monte Carlo methods enable the extraction of pair-potentials from the pair-correlation function,  $g(r)$ , of stable semi-dilute dispersions of identical particles [6, 12, 13]. This method assumes pair-wise additivity of potentials [14] and is difficult to implement without introducing artifacts from confining surfaces. All of

these equilibrium methods are limited to interactions of less than a few  $k_B T$ . An alternative approach, due to Crocker and Grier [15], analyzes the dynamics of a system relaxing toward equilibrium. Their method, Markovian Dynamics Extrapolation (MDE), offers the attractive advantage of sampling higher interaction energies by driving the system out of equilibrium with an external force. MDE elegantly identifies the equilibrium distribution,  $P_{eq}$ , as an eigenvector (with eigenvalue one) of the experimentally sampled finite-time propagator. However, forces are not extracted from local properties of the trajectories. Rather, the propagator must be thoroughly sampled over the full range of the interaction - from hardcore repulsion at short-range to zero force at long-range. Furthermore, systematic effects due to sampling errors on the calculation of the eigenvectors are hard to quantify and artifacts from hydrodynamics are difficult to rule-out.

In this Letter, we present a simple method for extracting conservative forces between isolated pairs of colloidal particles from the statistics of their trajectories at short time intervals. While our experimental apparatus is a straight-forward extension of the blinking optical tweezers introduced by Crocker and Grier [15], we introduce an alternative method of data analysis that implicitly accounts for hydrodynamic coupling and makes no assumptions about the form of conservative forces. We apply this method to characterize the electrostatic interactions of polymer colloids suspended in a nonpolar microemulsion.

We measure the electrostatic interactions of carboxylate modified polystyrene latex particles, radius  $a = 600$  nm (Interfacial Dynamics Corp.), suspended at vanishingly small volume fraction,  $\phi = 10^{-6}$ , in a nonpolar microemulsion of AOT (sodium di-2-ethylhexylsulfosuccinate) in hexadecane. A glass chamber, constructed from a standard microscope slide, three

microscope coverslips (No 1.5), and UV curing epoxy (Norland 61), holds the sample for optical microscopy and micromanipulation. An inverted optical microscope (Nikon TE2000) equipped with an oil immersion lens (100X, N.A. 1.4) images the suspension in brightfield. Images are recorded on a high speed digital video camera (Photron Fastcam 1024PCI) at a frame rate of 500Hz. Centroid algorithms [16], implemented in MATLAB, locate particle centers to a resolution of about 10 nm.

We extract interparticle forces from the statistical properties of the trajectories of isolated pairs of beads. We use blinking optical tweezers [15] to repeatedly trap and release particles at a desired separation. This method allows us to efficiently acquire good statistics for the trajectories of spheres in unlikely configurations. In our setup, described elsewhere [17], a pair of optical traps is made with the 532nm output of a diode-pumped solid state laser (Coherent Verdi V-5) using holographic optical tweezers [18, 19, 20]. To avoid wall effects [21, 22, 23], particles are trapped at least 10 $\mu$ m from the walls of the sample chamber. Once the optical tweezers have set the height and initial separation of the beads, we blink the laser using a chopper (Thorlabs MC1000A) at a rate  $1/\tau = 20$  Hz, with a duty cycle of 1:6. While the laser is off, the particles move freely, traveling distances up to about 200 nm. This motion is a combination of thermal diffusion and drift induced by interparticle forces. As the solvent does not absorb a measurable amount of trapping light, we expect that local heating by the optical tweezers is not significant. Furthermore, if any heat were delivered by the laser, it would be dissipated within microseconds by thermal conduction. By studying the motions of the particles only when the trap is off, we ensure that our measurements are insensitive to the details of the interaction of the trap with the particles and to any interactions between particles due to light scattering in the traps [24].

We construct time-dependent two-particle probability distributions from trajectories of free particles. Each recorded image, as shown in Figure 1(a), yields a value of the interparticle separation  $r$ . From these values, we tabulate a list of all statistically independent pairs of initial and final separations for a given time interval,  $\Delta t$ . While we only analyze time intervals between laser flashes, we concatenate data across all blinks and assign each event to a spatial bin according to its average separation  $(r_i + r_f)/2$ . We select the bins so that all bins contain 15000 events. Finally, for each spatial bin and time interval,  $\Delta t$ , we count the number of events with a particular value of displacement  $\Delta r$ ,  $N(r, \Delta r, \Delta t)$ . Histograms for different values of  $\Delta t$  at an average separation  $r = 2.04 \mu\text{m}$  are plotted in Figure 1(b). Each histogram represents the time-dependent two-particle probability distribution, and is well-fit by a Gaussian curve. The position of the center and width of these distributions increase linearly with time, as shown in Figure 1(c). The slope of the

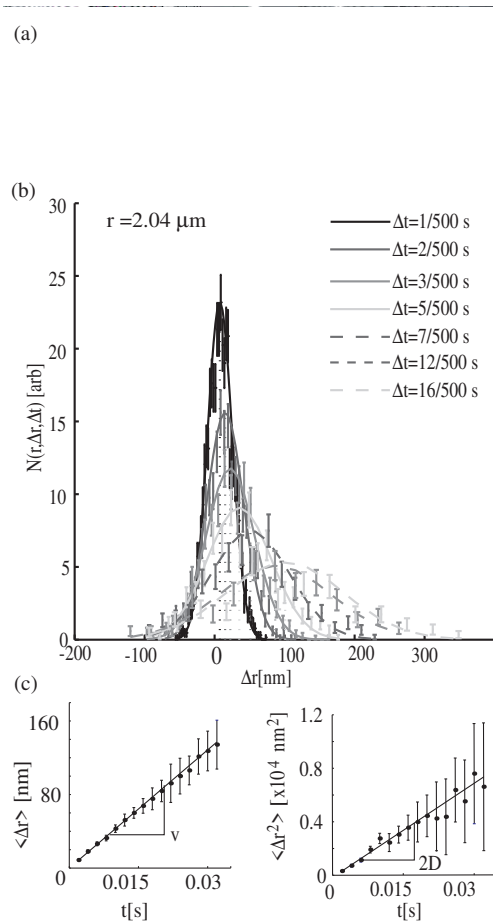


FIG. 1: Statistics of Particle Trajectories at Short Time-Intervals (a) Typical images of trapped and free CML beads ( $a=600$  nm) in 1 mM AOT/hexadecane. (b) A histogram of  $\Delta r$  at various  $\Delta t$  is plotted for an average separation  $r = 2.04 \mu\text{m}$ . (c) Plotting the mean displacement and the mean squared-displacement as a function of time, we extract two transport coefficients  $v$  and  $D$  respectively.

mean displacement provides a drift velocity,  $v$ . Likewise, the slope of the mean squared-displacement provides a diffusion coefficient,  $D$ . We observe these linear relationships at all particle separations. The spatial dependence of the velocity and diffusion coefficients are plotted in Figure 2. The relative velocity is positive and decreases slowly from a maximum at the smallest separation, clearly demonstrating a long-range repulsive force. Similarly, the diffusion is suppressed as particles come near contact. At low Reynolds number, force and velocity are related through the hydrodynamic mobility,  $v = bF$ . The mobility,  $b$ , generally depends on the size and separation of the spheres and the viscosity of the solvent. If the particles and solvent have been characterized in separate experiments, then the mobility can

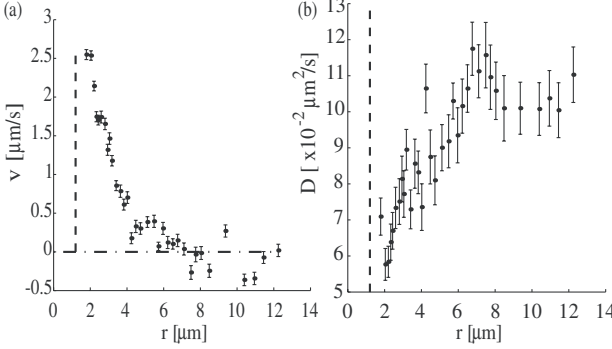


FIG. 2: Separation dependence of (a)  $v(r)$ , the mean velocity of separation, and (b)  $D(r)$ , the relative diffusion coefficient. This data was taken with CML beads ( $a=600$  nm) in 1mM AOT/hexadecane.

be calculated from existing theory [25]. However, typical expressions for hydrodynamic mobility are complicated by the presence of surface charge and counterions [26]. Without *a priori* knowledge of the zeta potential and screening length, these challenging calculations become intractable. We sidestep this obstacle by exploiting our simultaneous measurement of the relative velocity and diffusion coefficients.

To clarify the relationship between the transport coefficients and forces, let us consider a generalized form of Fick's first law for a system of  $N$  interacting particles [27]:

$$\vec{J}_i = -\bar{D}_{ij} \cdot [\vec{\nabla}_j P + \beta(\vec{\nabla}_j U)P]. \quad (1)$$

Here,  $\vec{J}_i$  is the probability current of the  $i^{\text{th}}$  particle,  $\bar{D}_{ij}$  is the diffusivity tensor,  $P = P(\vec{r}_1, \dots, \vec{r}_N, t)$  is the probability distribution,  $\beta = 1/k_B T$ , and  $U(\vec{r}_1, \dots, \vec{r}_N)$  is the potential energy. We use Einstein notation, where repeated indices imply summation. The first term in Equation [1] is the current due to coupled diffusion and the second term captures drift due to conservative forces. Enforcing the conservation of probability, we arrive at the Smoluchowski equation:

$$\partial_t P = -\vec{\nabla}_i \cdot \vec{J}_i = \vec{\nabla}_i \cdot \bar{D}_{ij} \cdot [\vec{\nabla}_j P + \beta(\vec{\nabla}_j U)P]. \quad (2)$$

The Onsager relations [28] demand that,  $\bar{D}_{ij} = \bar{D}_{ji}$ . Therefore,  $\bar{D}_{ij}$  can be diagonalized by a set of normal coordinates,  $\vec{x}_1 \dots \vec{x}_N$ . If the interaction potential is a linear combination of contributions from each mode,  $U = \sum_i U_i(\vec{x}_i)$ , then the probability distribution can be separated,  $P = \prod_i P_i(\vec{x}_i)$ , and

$$\partial_t P_i = \vec{\nabla}_i \cdot [\bar{D}_i \cdot \vec{\nabla}_i P_i - \vec{u}_i P_i], \quad (3)$$

where  $\vec{u}_i = -\beta \bar{D}_i \cdot \vec{\nabla}_i U_i$ . The spatial dependence of  $\bar{D}_i$  and  $\vec{u}_i$  complicate the direct application of Equation [3] to data. To make it tractable, we exploit the fact that

we are sampling the system only over short time intervals,  $\tau$ . The transport coefficients are effectively constant provided that:  $\langle \Delta x_i(\tau) \rangle u'_i \ll u_i$ ,  $\sqrt{\langle \Delta x_i(\tau)^2 \rangle} u'_i \ll u_i$ ,  $\langle \Delta x_i(\tau) \rangle D'_i \ll D_i$ , and  $\sqrt{\langle \Delta x_i(\tau)^2 \rangle} D'_i \ll D_i$ , where primed variables indicate spatial derivatives. Furthermore, the vector nature of the normal modes can be ignored provided that their displacements are small compared to their magnitude:  $\langle \Delta x_i(\tau) \rangle \ll x_i$  and  $\sqrt{\langle \Delta x_i(\tau)^2 \rangle} \ll x_i$ . This leads to a tractable one-dimensional form for the Smoluchowski equation:

$$\dot{P}_i = D_i P''_i - (u_i - D'_i) P'_i. \quad (4)$$

This is exactly solved by a Gaussian distribution,

$$P(\Delta x_i, \Delta t) = \frac{1}{\sqrt{2\pi \langle \Delta x_i^2 \rangle}} e^{-\frac{(\Delta x_i - \langle \Delta x_i \rangle)^2}{2\langle \Delta x_i^2 \rangle}}, \quad (5)$$

where the mean displacement

$$\langle \Delta x_i \rangle = v_i \Delta t = (u_i - D'_i) \Delta t, \quad (6)$$

defines the drift velocity,  $v_i$ , of the normal mode and the mean squared-displacement  $\langle \Delta x_i^2 \rangle = 2D_i \Delta t$ . Rearranging Equation 6, we arrive at a convenient expression for the conservative force acting on the  $i^{\text{th}}$  normal mode,

$$F_i = -U'_i = k_B T \left( \frac{v_i}{D_i} + \frac{D'_i}{D_i} \right). \quad (7)$$

Thus, we can simply extract the force from locally measured transport coefficients without appealing to a particular model of hydrodynamic or conservative forces.

This analysis is readily applied to identical colloidal particles, where the separation vector  $\vec{r}$  is a normal mode for the diffusion tensor and  $U = U(\vec{r})$ . In our data, the contribution from the second term in Eq. 7 is negligible, so the interparticle force reduces to  $F(r) = k_B T v(r)/D(r)$ . Directly dividing the velocities by the diffusivities at each separation found in Figure 2, we arrive at the force profile shown in Figure 3. These spheres show purely repulsive interactions with a maximum measurable force of about 100 fN and a resolution of a few fN. The interparticle forces fall off slowly as the particle separation increases, with measurable repulsions out to about five particle diameters. These results are well-fit by a screened-Coulomb form,

$$F(r) = k_B T \left( \frac{e\zeta}{k_B T} \right)^2 \frac{a^2}{\lambda_B} \frac{e^{-\kappa(r-2a)}}{r} \left( \frac{1}{r} + \kappa \right), \quad (8)$$

where the Bjerrum length  $\lambda_B = e^2/4\pi\epsilon_0 k_B T$ . This fit returns a screening length  $\kappa^{-1} = 5.0 \pm 0.2 \mu\text{m}$  and an apparent surface potential,  $|e\zeta/k_B T| = 3.30 \pm 0.04$ . It is important to note that the fitted value of  $|e\zeta|$  reflects the surface potential as seen from long-range. This value will be smaller than the actual surface potential for highly

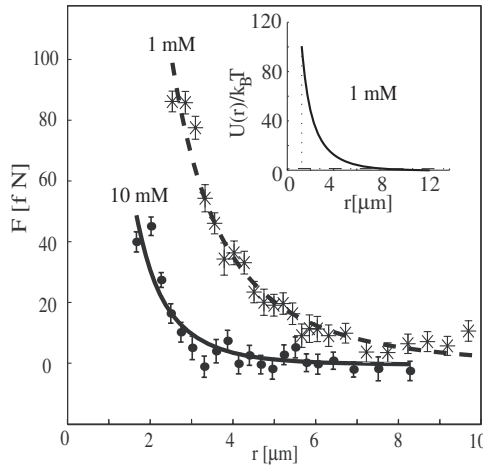


FIG. 3: Electrostatic forces between charged colloidal particles in a nonpolar solvent. Repulsion between carboxylate modified PS at two concentrations of AOT, as noted. Curves are fits to screened-Coulomb interactions (inset) Interaction energy,  $U(r)/k_B T$ , implied from a fit at 1 mM AOT.

charged surfaces due to non-linear screening near the particle surface.

As expected, the interparticle forces vary with the concentration of surfactant [6]. When the concentration of AOT is increased to 10 mM, the range and scale of the interparticles forces drop, as shown in Fig. 3. In particular, the screening length is lowered to  $0.6 \pm 0.1 \mu\text{m}$  and the apparent surface potential is significantly reduced  $|e\zeta/k_B T| = 1.8 \pm 0.1$ .

Interaction potentials,  $U(r)$ , can be calculated from these these parameters, as demonstrated in the inset of Figure 3. The potential is soft and long-ranged, decaying from about  $100 k_B T$  at contact to  $< k_B T$  at about  $r = 10 \mu\text{m}$ . We use fitted values of  $\kappa^{-1}$  and  $|e\zeta/k_B T|$  because we have found direct integration of the force curve to be highly unreliable; by simply varying the size of the spatial bins, conventional potentials with screened-Coulomb forms can be transformed into anomalous potentials with long-range attractions.

We present a powerful method for extracting the conservative forces between colloidal particles from the statistics of their trajectories. This method requires no separate measurements of solvent and particle properties. The only supporting measurements are the spatial calibration of the imaging system, the temporal calibration of the high-speed camera and the temperature of the system. Additionally, our measurement is completely independent of specific models for hydrodynamic and electrostatic interactions between particles. Our method of data analysis, rooted in the general principles of nonequilibrium statistical mechanics, may be extended to probe generalized forces acting on fluctuating normal modes of any thermal system, from more complex colloidal systems to the internal dynamics of molecules.

We thank Ian Morrison and Todd Squires for helpful discussions and Cabot Corporation for support.

\* Electronic address: eric.dufresne@yale.edu

- [1] B. V. Derjaguin and L. Landau, *Acta Physicochim. USSR* **14**, 633 (1941).
- [2] E. J. W. Verwey and J. T. G. Overbeek, *Theory of the Stability of Lyophobic Colloids: The Interactions of Sol Particles Having an Electric Double Layer* (Elsevier, 1948).
- [3] I. D. Morrison, *Colloids and Surf. A* **71**, 1 (1993).
- [4] W. H. Briscoe and R. G. Horn, *Langmuir* **18**, 3945 (2002).
- [5] C. E. McNamee, Y. Tsujii, and M. Matsumoto, *Langmuir* **20**, 1791 (2001).
- [6] M. F. Hsu, E. R. Dufresne, and D. A. Weitz, *Langmuir* **21**, 4881 (2005).
- [7] W. H. Briscoe and P. Attard, *Journal of Chemical Physics* **117**, 5452 (2002).
- [8] J. Israelachvili, *Intermolecular and Surface Forces* (Elsevier, London, 1992).
- [9] W. A. Ducker, T. J. Senden, and R. M. Pashley, *Nature* **353**, 239 (1991).
- [10] D. C. Prieve and N. A. Frej, *Langmuir* **6**, 396 (1990).
- [11] P. L. Biancaniello and J. C. Crocker, *Rev. Sci. Inst.* **77**, 113702 (2006).
- [12] G. M. Kepler and S. Fraden, *Phys. Rev. Lett.* **73**, 356 (1994).
- [13] S. H. Behrens and D. G. Grier, *Phys. Rev. E* **64**, 050401(R) (2001).
- [14] M. Brunner, C. Bechinger, W. Strepp, V. Lobaskin, and H. von Grunberg, *Europhys. Lett.* **58**, 296 (2002).
- [15] J. C. Crocker and D. G. Grier, *Phys. Rev. Lett.* **73**, 352 (1994).
- [16] J. C. Crocker and D. G. Grier, *J. Colloid Interface Sci.* **179**, 298 (1996).
- [17] S. C. Chapin, V. Germain, and E. R. Dufresne, *Optics Express* **14** (2006).
- [18] E. R. Dufresne and D. Grier, *Rev. Sci. Inst.* **69**, 1974 (1998).
- [19] E. R. Dufresne, G. C. Spalding, M. T. Dearing, S. A. Sheets, and D. G. Grier, *Rev. Sci. Inst.* **72**, 1810 (2001).
- [20] J. Liesener, M. Reicherter, T. Haist, and H. J. Tiziani, *Opt. Comm.* **185**, 77 (2000).
- [21] A. E. Larsen and D. G. Grier, *Nature* **385**, 230 (1997).
- [22] E. R. Dufresne, T. M. Squires, M. P. Brenner, and D. G. Grier, *Phys. Rev. Lett.* **85**, 3317 (2000).
- [23] T. M. Squires and M. P. Brenner, *Phys. Rev. Lett.* **85**, 4976 (2000).
- [24] M. M. Burns, J. M. Fournier, and J. A. Golovchenko, *Phys. Rev. Lett.* **63**, 1233 (1989).
- [25] G. K. Batchelor, *J. Fluid. Mech.* **74**, 1 (1975).
- [26] R. W. O'Brien and L. R. White, *J. Chem. Soc. Faraday Trans. II* **74**, 1607 (1978).
- [27] J. K. G. Dhont, *An Introduction to Dynamics of Colloids* (Elsevier, 1996).
- [28] R. K. Pathria, *Statistical Mechanics* (Butterworth-Heinemann, 1996), 2nd ed.